

Veronika Beck^{1,2,*}, Nikolai Dotzek², Robert Sausen²

¹ Physik-Department, Technische Universität München, Garching, Germany

² Deutsches Zentrum für Luft- und Raumfahrt (DLR), Oberpfaffenhofen, Germany

1. INTRODUCTION

Tornado intensities are usually determined according to the damage produced by the tornadoes. Here, a method for the reconstruction of tornado near-surface wind fields and their intensity from forest damage is described. Forest damage due to tornadoes has already been documented by Wegener (1917), Letzmann (1923), Budney (1965) and Fujita (1985) while Holland et al. (2006) (cf. Dotzek et al., 2008) focussed on the simulation of forest damage patterns by using a simple vortex model. A model based on the analytical tornado wind field model of Letzmann (1923) (cf. Dotzek et al., 2000) and a mechanistic tree model of Peltola and Kellomäki (1993) was developed in order to simulate real tornado forest damage patterns. From the comparison of the simulated and real forest damage patterns, conclusions on the tornado intensity and important parameters of the tornado near-surface wind field can be drawn. Full details are given in Beck (2008).

2. ANALYTICAL TORNADO MODEL OF LETZMANN (1923)

Letzmann (1923) developed a three-dimensional analytical tornado model with a linear velocity increase in the tornado core and hyperbolic velocity decay in the tornado mantle. The equations for the tangential and radial velocity component (v_θ and v_r) are similar to those of a Rankine vortex (Fig.1) with R_{\max} indicating the radius of the tornado core:

$$\begin{aligned} v_{r,\theta} &= v_{r,\theta\max} (r / R_{\max}) & r \leq R_{\max} \\ v_{r,\theta} &= v_{r,\theta\max} (R_{\max} / r)^\gamma & r \geq R_{\max} \end{aligned} \quad (1)$$

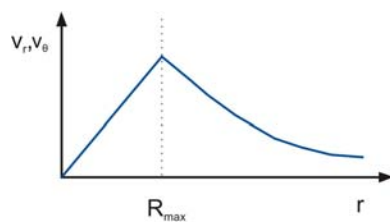


Figure 1: Radial and tangential velocity distribution of a Rankine vortex with a linear increase of velocity in the tornado core ($r < R_{\max}$) and a hyperbolic decay with an exponent γ of velocity in the mantle ($r > R_{\max}$).

* Corresponding author address: Veronika Beck, Physik-Department T34, Technische Universität München, D-85748 Garching, Germany; e-mail: veronika.johanna.regina.beck@mytum.de.

The exponent γ is set to $\gamma = 1.0$ and a constant translation speed v_{trans} of the tornado in y-direction is assumed. In contrary to other mathematical descriptions of the Rankine-vortex (Kanak, 2005), the radial v_r and tangential velocity components v_θ of the vortex depend on the three parameters v_{trans} , G_{\max} and α . Here, G_{\max} indicates the ratio between circular v_{cir} and translation velocity component v_{trans} of the tornado wind field and α is the angle between the direction of the wind and the pressure gradient at the point of maximum velocity.

The dependence of the velocity field of the Rankine vortex on the parameters G_{\max} and α show some interesting effects (Fig.2). By varying the parameter G_{\max} for $G_{\max} < 1.0$, no calm points occur (a) while at $G_{\max} = 1.0$ one central calm point is notable (b) and for $G_{\max} > 1.0$ two calm points are visible, one central calm point and one marginal calm point (c). The distance between these two calm points grows for increasing values of $G_{\max} > 1.0$. The resulting plots of the variation of the angle α are illustrated in Fig. 2 (d)-(f). For $|\alpha| < 90^\circ$, radial and spiral inflow into the vortex center is notable (a), while for $|\alpha| = 90^\circ$ concentric circles occur around the vortex center, i.e. the central calm point, (b). Increasing the angle α , spiral and radial outflow of the central calm point is visible for $|\alpha| > 90^\circ$.

Further on, Letzmann (1923) discussed the possibility of a variation of the angle α within the velocity field and defined a tornado core to be "genuine" or "false". A genuine core in two dimensions has outflow from the vortex center and inflow from the outside (Fig. 4a2) leading to a two-cell vortex (cf. Sullivan vortex). This effect is achieved by varying the angle α from $\alpha = \pi$ at the vortex center over $\alpha = -90^\circ$ at the borderline between tornado core and tornado mantle ($r = R_{\max}$) and $\alpha = 0^\circ$ outside the tornado wind field (Fig. 4a1). Hence, a false core is defined by spiral inflow into the vortex center and inflow from the outside (Fig. 4b2). Fig. 4b1 shows a false core and was produced by varying the angle α from $\alpha = 0^\circ$ at the vortex center to $\alpha = -90^\circ$ at $r = R_{\max}$ and $\alpha = 0^\circ$ outside the tornado wind field. According to Letzmann (1923), during a tornado life cycle the behaviour of a tornado core changes from a false core to a genuine core at its mature stage.

Furthermore, Letzmann (1923) derived theoretical tree damage patterns for different values of the parameters α and G_{\max} depending on the critical intensity for stem breakage of the trees. For

this, he introduced a falling angle ψ indicating the deviation of the falling direction of the trees from the direction of the translation velocity component of the tornado wind field. According to Letzmann (1923), a tree with $\psi = 0^\circ$ indicates either a converging or a diverging line, while a tree with $\psi = 180^\circ$ characterizes a converging line. The tree with $\psi = 180^\circ$ is only found for values of $G_{\max} \geq 2.0$. Letzmann (1923) classified the theoretical tree damage patterns into four swath types. Fig. 5 shows the numerically reproduced theoretical tree damage patterns and the corresponding streamline patterns of Letzmann (1923). For $|\alpha| > 90^\circ$, all swath types have the same divergent damage pattern, while for $|\alpha| \leq 90^\circ$ the behaviour of the theoretical damage patterns is different. Swath type I displays damage patterns with converging trees into the center. This swath type occurs for values of $G_{\max} < 1.0$ and low intensities. Swath type II is found for G_{\max} between 1.0 and 3.5 for low and moderate intensities. The converging line ($\psi = 0^\circ$) moves to the left with increasing absolute value of α . Swath type III is obtained for slow-moving tornados with high intensities however, the values of G_{\max} correspond to that of swath type II. Swath type IV indicated by a tree with $\psi = 180^\circ$ is found for high values for G_{\max} especially for tornadoes with huge circulation or very slow translation velocity.

3. STRUCTURE OF THE MODEL

The model for the simulation of tree damage patterns consists of a wind field model for a tornado near-surface wind field and a tree model for the calculation of the critical velocity of the trees for stem breakage. The structure of the model is outlined in Fig. 3. The analytical tornado model of Letzmann (1923) serves as wind field model. In the first part of the model, the critical velocity for stem breakage is derived from the mechanistic HWIND model of Peltola and Kellomäki (1993). Here, either a random or homogeneous distribution of trees can be used. The bending moment and the tree resistance are calculated from several tree parameters with an initial velocity guess and the values are compared. If the bending moment exceeds the tree resistance the iteration ends, otherwise the velocity is increased by 0.5 ms^{-1} steps.

The calculations are done for a $400 \text{ m} \times 400 \text{ m}$ domain with a grid size of 10 m in each direction and cut-off at the border of the domain. The file containing the critical velocity is read into the wind field program to simulate the tree damage patterns. The wind field model produces an instantaneous velocity at each grid point which is compared to the critical velocity for stem breakage. If the instantaneous velocity exceeds the critical velocity for stem breakage the tree is considered to be broken and the falling direction is assumed to be the instantaneous direction of the wind field at the

corresponding point. Either the wind field model or the tree model can be substituted by another tree model (e.g. the Gales model of Gardiner et al. (2000)) or another tornado wind field (e.g. Rankine vortex with weaker hyperbolic decay with $\gamma < 1$, Burgers-Rott vortex).

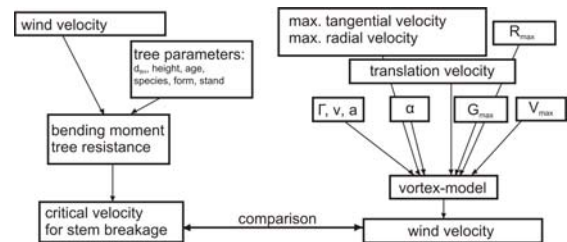


Figure 3: Structure of the complete model consisting of the tree model for the calculation of the critical velocity for stem breakage and the wind field model which gives the instantaneous wind velocity at each grid point. If the instantaneous wind velocity exceeds the critical velocity the tree is considered to be broken.

4. FOREST DAMAGE ANALYSIS: THE F3-TORNADO OF MILOSOVICE, 31 MAY 2001

The tornado of Milosovice, Czech Republic, occurred on 31 May 2001 with a path width of 400 – 500 m and an estimated path length of 4.5 km. According to Martin Setvák from the Czech Weather Service CHMI, beside the main vortex (1), three smaller vortices (2), (3) and (4) have been observed. The tornado was classified as an F3 tornado (ESWD database). The aerial photo of the forest damage (Fig. 6a) was taken by Martin Setvak and divided into four parts for the damage patterns of the single vortices. From radar observations, the translation speed of the thunderstorm cell producing the tornado is estimated as 16.5 ms^{-1} .

The damage patterns of the single vortices are analyzed by different parameters. First, an estimation of the angle α is made by analyzing if the damage pattern is convergent or divergent. Then, the value of G_{\max} has to be derived from the damage patterns in the same way as the sense of rotation of the vortex (cyclonic or anticyclonic), the radius R_{\max} of the tornado core and the type of the tornado core (Rankine vortex, etc.) by comparison of simulated damage patterns with the real damage patterns by varying the single parameters. From these parameters the near-surface wind fields of the vortices can be reconstructed.

Fig. 7 demonstrates the damage pattern analysis of the main tornado. The damage patterns show a mainly divergent damage patterns resulting in an angle α of $|\alpha| > 90^\circ$. By varying the other parameters G_{\max} and R_{\max} the real damage pattern is approached by consecutive simulations. On the left side of (a), a dominating tangential flow is pointed out by a notable effect of the tornado mantle, while on the right side the divergent behaviour of the damage patterns is predominant. The simulated damage pattern of (a) is obtained by

setting $G_{\max} = 5.0$, $\alpha = 140^\circ$ and the radius of the core at $R_{\max} = 80$ m. The Fujita-scale distribution indicates an F4 zone in the middle of the damage path and a widespread F3 zone for this simulation.

The parameters of the simulation concerning (b) were set to $G_{\max} = 4.0$, $\alpha = 140^\circ$ and $R_{\max} = 80$ m due to a lower tangential velocity component. According to a smaller maximum velocity, the damage pattern corresponds to a tornado having mainly F3 and F2 regions. Compared to the simulation in (b), a stronger divergence on the right border of the domain occurs for (c). Therefore, α is set to -150° in order to obtain a damage pattern with stronger divergence. G_{\max} and R_{\max} retain the same values as in (b). The Fujita-scale distribution of the simulation of (c) outlines a tornado with dominating F3 region. From this simulation and the estimation of the translation speed of the tornado from radar observations, the maximum velocity of the tornado is derived by using the relation

$$G_{\max} = V_{\text{cir}} / V_{\text{trans}} \quad (2)$$

region	G_{\max}	α [°]	R_{\max} [m]	type	v_{trans} [m s ⁻¹]	v_{cir} [m s ⁻¹]	v_{max} [m s ⁻¹]
Ia	5.0	-140	80	Rank	16.5 ± 1.0	82.5 ± 5.0	99.0 ± 6.0
Ib	4.0	-140	80	Rank	16.5 ± 1.0	55.5 ± 4.0	82.5 ± 5.0
Ic	4.0	-150	80	Rank	16.5 ± 1.0	55.5 ± 4.0	82.5 ± 5.0
IIa	1.5	160	80	Rank	9.8-17.8	14.8-26.7	24.7-44.5
IIb	1.5	180	80	Rank	9.8-17.8	14.8-26.7	24.7-44.5
IIc	1.0	180	80	Rank	12.3-22.3	12.3-22.3	24.7-44.5
IIIa	1.0	0	40	ca II	12.4-22.3	12.4-22.3	24.7-44.5
IIIb	2.5	-90	40	Rank	7.1-12.7	17.6-31.8	24.7-44.5
IIIc	4.0	-90	60	ca II	4.9-8.9	19.8-35.6	24.7-44.5
IVa	4.0	150	60	Rank	4.9-8.9	19.8-35.6	24.7-44.5
IVb	4.0	120	60	Rank	4.9-8.9	19.8-35.6	24.7-44.5

Table 1: Parameters and velocity components gained through the damage analysis for the single vortices of the tornado of Milosovice, CZ.

The translation velocity component of the tornado can be determined with an uncertainty of ± 1.0 m s⁻¹. Therefore, the maximum velocity of the tornado wind field is calculated with a maximum error of 10 m s⁻¹. This means, that a determination of the maximum wind speed of the tornado within half a level of the Fujita-scale is possible. For the three smaller vortices, no maximum velocity could be determined since the translation velocity component is unknown and can not be estimated from radar observations. Therefore, the velocities illustrated in Table 1 are a lower limit of the possible velocities that have been derived from the critical velocity of stem breakage from the HWIND model. All vortices, including the main tornado are outlined with their traces (dashed lines) and the diverging or converging lines (dashed-dotted lines) in Fig. 6b. For vortex 1, 2 and 4, the diverging line is indicated by trees with $\psi = 0^\circ$ in the corresponding damage patterns. Regarding vortex 1 and 4, the diverging line is located right resp. left of the trace of the tornado, while for vortex 2, the trace and the diverging line coincide. For vortex 3, the trees with $\psi = 0^\circ$ here indicate a converging line that coincides with the trace of the vortex.

Fig. 8 illustrates the corresponding reconstructed near-surface wind fields of the

different tornado vortices. The main vortex (Ia-Ic) is characterized by spiral outflow and a high G_{\max} . Vortex 2 (IIa-IIc) shows a smaller G_{\max} and anticyclonic rotation. The wind field of this vortex is also dominated by outflow of the tornado core. The different reconstructed wind fields of vortex 3 show parts of the evolution of a tornado life cycle. While the near-surface wind fields of vortex 4 (IVa-IVb) are similar to that of the main vortex but with smaller extension and anticyclonic rotation.

The damage patterns could be reproduced by simulations mainly using the Rankine vortex. This indicates that the tornado near-surface wind field reconstructed from damage patterns is described best by the velocity profile of a Rankine vortex with linear velocity increase inside the tornado core and hyperbolic velocity decay in the tornado mantle. For the main vortex, a value of $G_{\max} = 4.0 - 5.0$ was found verifying the observations of Letzmann (1925) who calculated values of $G_{\max} = 6.0$ for tornadoes in the United States of America and Europe. The range $120^\circ < |\alpha| < 180^\circ$ is consistent to the descriptions of Letzmann (1923) for divergent damage patterns. The derived maximum velocity of the main tornado (1) lies in the region of an F3 or F4 tornado. Two of three damage patterns result in a F3 tornado and severe damage due to F4 intensity occurs only on a few points. Thus, it can be said that this model verifies the classification of the tornado as a high F3 tornado, as rated in the ESWD database.

5. CONCLUSIONS

The above described model presents a method for the reconstruction of near-surface tornado wind fields from forest damage. The analytical tornado model of Letzmann (1923) depending on the parameters G_{\max} , α and V_{trans} suits perfectly for the determination of this parameters from the forest damage patterns. With the estimation of the translation speed of the tornado-producing thunderstorm cell from radar observations, the translation velocity component of the tornado can be determined. With the consecutive simulation of the forest damage patterns by varying the parameters G_{\max} , α and R_{\max} and the comparison to the real damage patterns, conclusions on the appearance of the near-surface tornado wind fields and the location of the trace of the tornado can be drawn. Compared to the determination of tornado intensities from damage, the maximum velocity of the tornado is determinable with an uncertainty of 10 m s⁻¹ corresponding to a half level of the Fujita-Scale. However, the advantage of this method is the possibility to reconstruct the tornado near-surface wind fields. In order to use this method for classification of tornadoes one has to be sure about vertical aerial photographs of the forest damage patterns, because otherwise it is very difficult to determine the location of the fallen trees exactly.

ACKNOWLEDGMENTS

This work was partly funded by the German Ministry for Education and Research (BMBF) under contract 01LS05125 in the project RegioExAKT (Regional Risk of Convective Extreme Weather Events: User-oriented Concepts for Climatic Trend Assessment and Adaptation, www.regioexakt.de) within the research programme klimazwei.

REFERENCES

- Beck, V., 2008: Near-surface tornado wind field reconstruction from forest damage. *Diploma thesis, TU München* 162pp.
- Budney, L. J., 1965: Unique damage patterns caused by a tornado in dense woodlands. *Weatherwise*, **18**, 75–77.
- Dotzek, N., G. Berz, E. Rauch, R. E. Peterson, 2000: Die Bedeutung von Johannes P. Letzmanns Richtlinien zur Erforschung von Tromben, Tornados, Wasserhosen und Kleintromben für die heutige Tornadoforschung. *Meteorol. Z.*, **9**, 165–174.
- Dotzek, N., R. E. Peterson, B. Feuerstein, M. Hubrig, 2008: Comments on “A simple model for simulating tornado damage in forests”. *J. Appl. Meteor. Climatol.*, **47**, 726–731.
- Fujita, T. T., 1989: The Teton-Yellowstone Tornado of 21 July 1987. *Mon. Wea. Rev.*, **117**, 1913–1940.

- Gardiner, B. A., H. Peltola, S. Kellomäki, 2000: Comparison of two models for predicting the critical wind speeds required to damage coniferous trees. *Ecol. Model.*, **129**, 1–23.
- Holland, A. P., A. J. Riordan, E. C. Franklin, 2006: A simple model for simulating tornado damage in forests. *J. Appl. Meteor. Climatol.*, **45**, 1597–1611.
- Kanak, K. M., 2005: Numerical simulation of dust devil-scale vortices. *Q. J. R. Meteorol. Soc.*, **131**, 1271–1292.
- Letzmann, J., 1923: Das Bewegungsfeld im Fuß einer fortschreitenden Wind- oder Wasserhose. *Dissertation, Acta Comm. Univ. Dorpat*, **AIII**, 1–136. www.essl.org
- Letzmann, J., 1925: Fortschreitende Luftwirbel. *Meteorologische Zeitschrift*, **42**, 41–52.
- Peltola, H., S. Kellomäki, 1993: A mechanistic model for calculating windthrow and stem breakage of Scots pines at stand edge. *Silva Fenn.*, **27**, 99–111.
- Wegener, A. L., 1917: Wind- und Wasserhosen in Europa. *Vieweg, Braunschweig*, 301pp. www.essl.org
- Tornado of Milosovice: <http://www.chmi.cz/torn/cases/20010531/20010531.htm> Accessed on 29 August 2008
- ESWD database: <http://www.essl.org/ESWD> Accessed on 29 August 2008

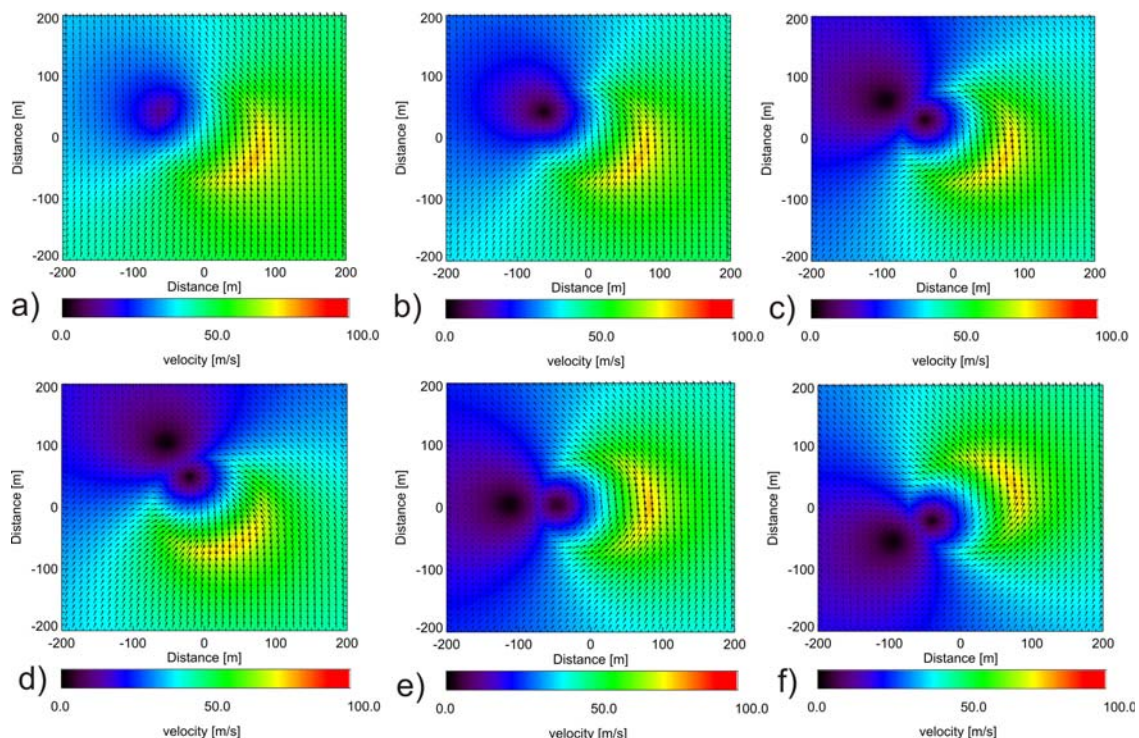


Figure 2: Wind fields for a constant angle $\alpha = 60^\circ$ and different values of $G_{\max} = 0.75$ (a), $G_{\max} = 1.0$ (b) and $G_{\max} = 1.5$ (c). The separation of the two calm points occurs at $G_{\max} = 1.0$. (d)-(f) show the wind fields for constant $G_{\max} = 1.5$ and different angles α ($\alpha = -30^\circ$ (d), $\alpha = -90^\circ$ (e) and $\alpha = -120^\circ$ (f)). Here, the change from spiral inflow into the vortex center to spiral outflow of the vortex center is demonstrated.

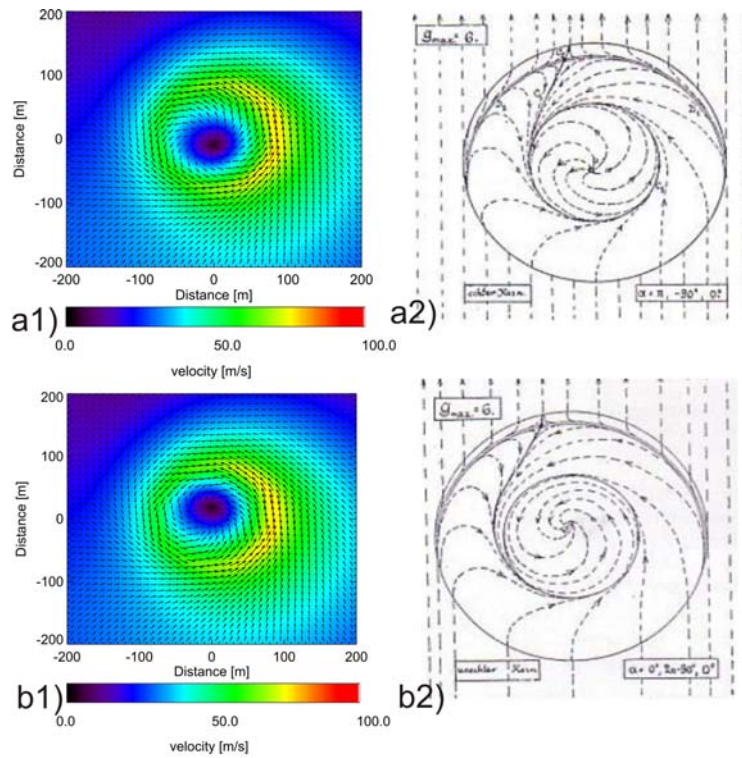
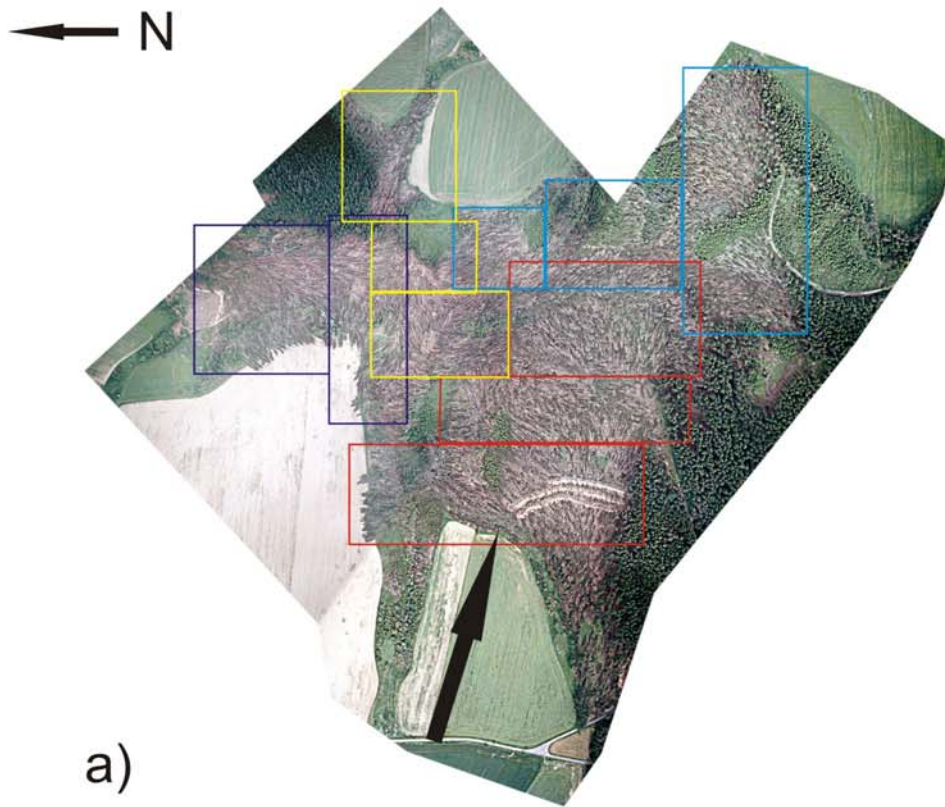


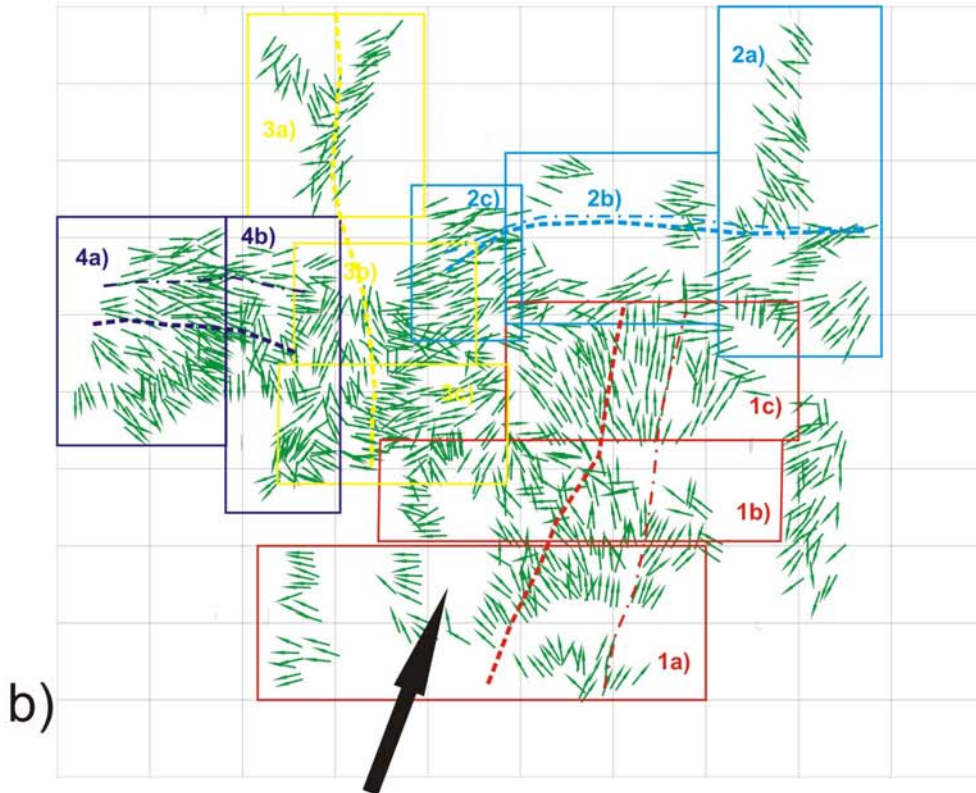
Figure 4: Genuine (a) and false (b) core for $G_{max} = 6.0$. The original graphics of Letzmann (1923) are shown on the right side while on the left side the numerically reproduced velocity fields are presented indicating spiral outflow from the vortex core for the genuine core and spiral inflow into the vortex core for the false core.

	Form a, $\alpha = 0^\circ$	Form b, $\alpha = -30^\circ$	Form c, $\alpha = -60^\circ$	Form d, $\alpha = -90^\circ$	
Type I					Form e, $\alpha = -135^\circ$
Type II					
Type III					Form f, $\alpha = 180^\circ$
Type IV					

Figure 5: Classification of the damage patterns into four different swath types depending on the angle α and G_{max} according to Letzmann (1923). G_{max} increases from swath type I to swath type IV.

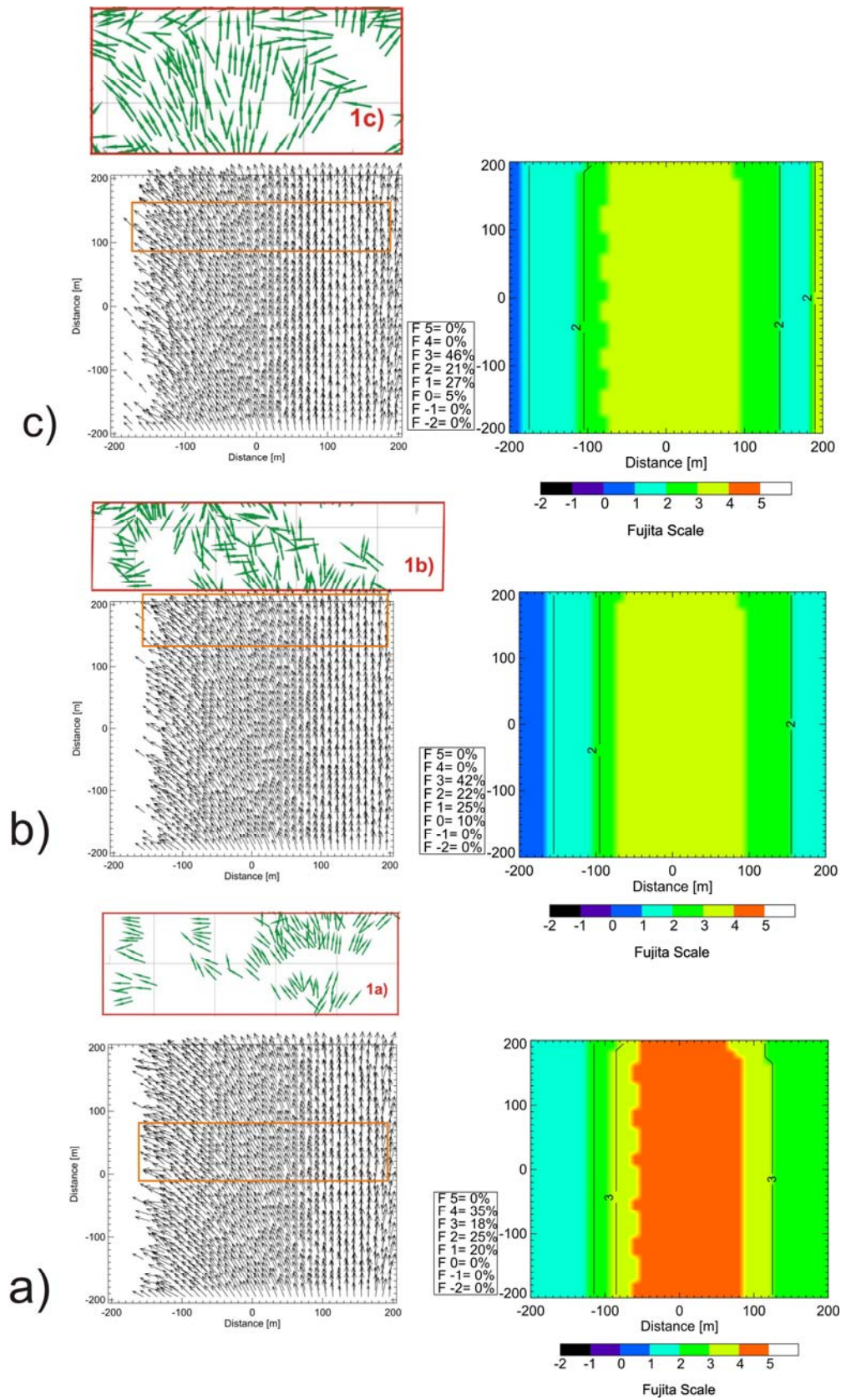


a)



b)

Figure 6: Aerial photograph of the forest damage produced by the tornado of Milosovice, CZ, (31 August 2001) (courtesy of Martin Setvak, CHMI) showing the division of the damage patterns into one main vortex (red) and three smaller vortices (a) and digitized damage patterns containing the trace (dashed line) and the diverging resp. converging line (dashed-dotted line) of the vortices (b).



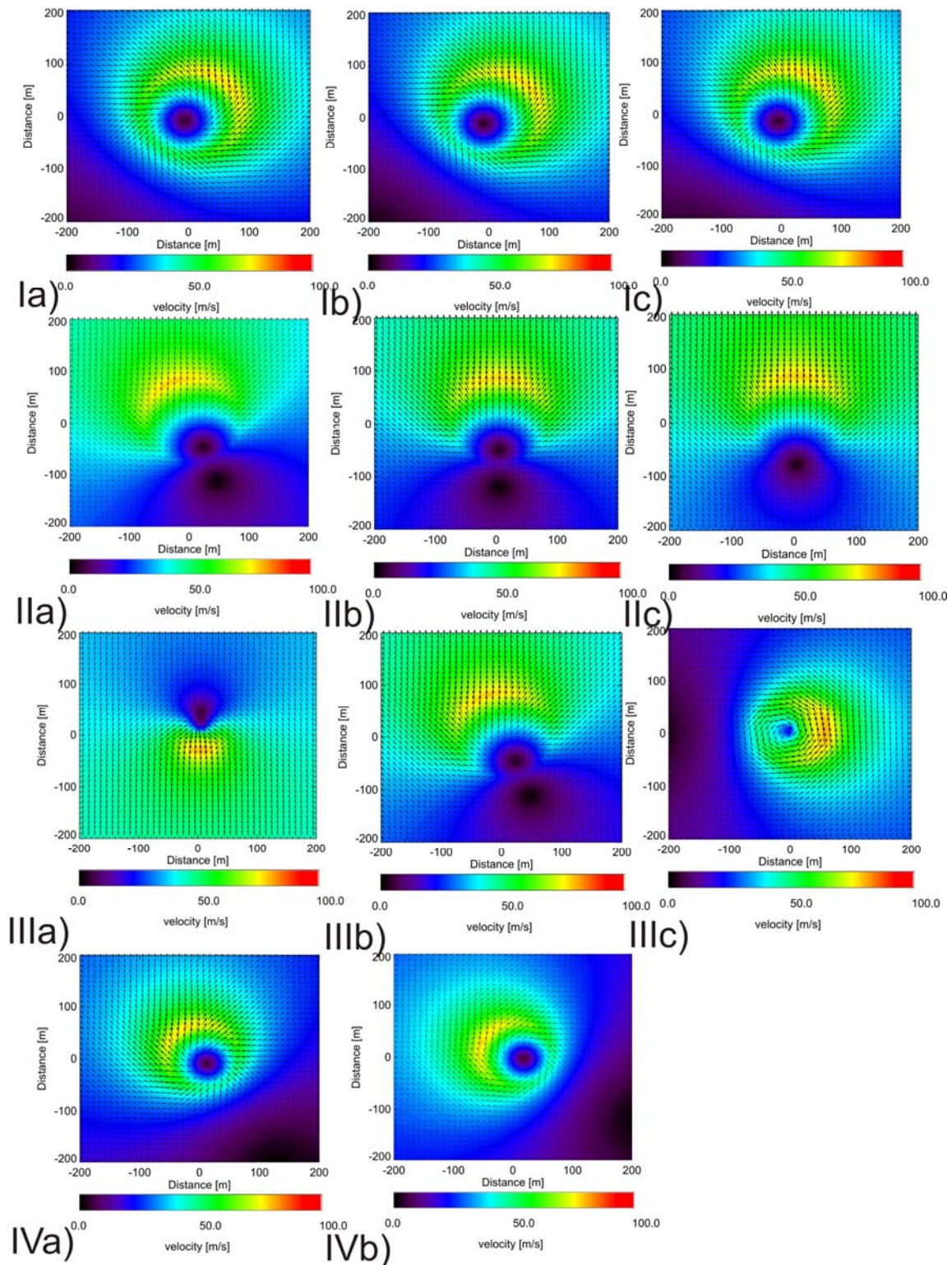


Figure 8: Reconstructed near-surface tornado wind fields from the forest damage patterns for the main vortex (I) and the three smaller vortices (II), (III) and (IV) indicating spiral outflow for the vortices (I), (II) and (IV). The vortices (I) and (III) have cyclonic sense of rotation while the vortices (II) and (IV) have anticyclonic sense of rotation. For the simulation the Rankine vortex was used.